

## Magnetotransport in the heavy-fermion system $\text{YbNi}_2\text{B}_2\text{C}$

A. Yatskar

*Department of Physics, University of California, Riverside, California 92521  
and National High Magnetic Field Laboratory, Los Alamos National Laboratory, Los Alamos, New Mexico 87545*

C. H. Mielke

*National High Magnetic Field Laboratory, Los Alamos National Laboratory, Los Alamos, New Mexico 87545*

P. C. Canfield

*Iowa State University and Ames Laboratory, Ames, Iowa 50011*

A. H. Lacerda

*National High Magnetic Field Laboratory, Los Alamos National Laboratory, Los Alamos, New Mexico 87545*

W. P. Beyermann

*Department of Physics, University of California, Riverside, California 92521*

(Received 22 October 1998)

We have measured the high field transverse magnetoresistance and magnetization on single crystalline samples of  $\text{YbNi}_2\text{B}_2\text{C}$  with the applied magnetic field both parallel and perpendicular to the  $c$  axis of the tetragonal crystal structure. At high temperatures, the magnetoresistance is negative with a magnitude that increases as the temperature is lowered. A scaling analysis of the data for  $\mathbf{H} \parallel \mathbf{c}$  finds a characteristic energy that is  $\sim 20$  K at low temperatures, which is a factor of 2 larger than the Kondo temperature determined from thermodynamic measurements, and it increases linearly with the temperature. Even though the magnetoresistance for  $\mathbf{H} \parallel \mathbf{c}$  is also negative, the data do not scale. At low temperatures, the magnetoresistance is very anisotropic. In the Fermi-liquid regime below  $\sim 1.6$  K, the resistivity has a temperature-independent contribution due to ligand and/or Kondo-hole disorder and a term from electron-electron scattering that goes like  $T^2$ . For  $\mathbf{H} \perp \mathbf{c}$ , the residual resistivity and the  $T^2$  coefficient are field dependent. Both the high- and low-temperature data are compared to various theoretical calculations. [S0163-1829(99)14631-9]

### I. INTRODUCTION

The borocarbides,  $R\text{Ni}_2\text{B}_2\text{C}$  ( $R = \text{Dy-Lu, Y}$ ), are an interesting series of compounds because of the interplay between superconductivity and magnetism in these systems.<sup>1</sup>  $\text{YbNi}_2\text{B}_2\text{C}$  is the anomalous member of the series in that no ordered ground state is observed down to  $\sim 50$  mK,<sup>2</sup> and in place of a broken symmetry there is a crossover to a heavy Fermi liquid at low temperatures.<sup>3</sup> A peak is observed in the magnetic contribution of the specific heat, and below the peak the temperature dependence is linear with a Sommerfeld coefficient of  $\sim 530$  mJ/mol K<sup>2</sup>. This feature is interpreted as a Kondo anomaly with an estimated Kondo temperature of  $\sim 10$  K.

Correlated-electron behavior is also observed in the magnetic susceptibility and electrical resistivity. The magnetic susceptibility is anisotropic and has a Curie-Weiss-like temperature dependence above  $\sim 150$  K. For the powder average, the effective moment is  $\sim 4\%$  larger than that calculated from the Hund's rule ground state for  $\text{Yb}^{3+}$ , and the Weiss temperature is  $\theta_{\text{av}} = -129.6$  K, indicating antiferromagnetic correlations are important at high temperatures. These correlations are responsible for the significant hybridization between the Yb  $4f$  levels and the conduction electrons at low temperatures where the susceptibility deviates from the Curie-Weiss behavior. Finally, the electrical resistivity

monotonically decreases with decreasing temperature, and below  $\sim 1.5$  K a Fermi-liquid regime develops with an enhanced  $T^2$  temperature dependence.

The temperature dependencies of these properties are prototypical of a Yb-based heavy-fermion compound where the spin-fluctuation temperature is well separated from the other energy scales that characterize the crystal-electric fields (CEF) and the vibrational excitations. Only a few Yb heavy-fermion compounds have been discovered, and unlike compounds such as  $\text{YbBiPt}$ ,<sup>4</sup> the largely separated energy scales ( $T_N, T_C \ll T_K \ll T_{\Delta\text{CEF}}$ ) in  $\text{YbNi}_2\text{B}_2\text{C}$  make this an ideal system for studying Kondo physics.

To investigate the magnetotransport of a heavy Fermi liquid, which is anomalously large in many heavy-electron compounds, we measured the transverse magnetoresistance both at high temperatures and in the low-temperature Fermi-liquid regime on single-crystalline  $\text{YbNi}_2\text{B}_2\text{C}$ . In Sec. II, the experimental procedure and results will be described. In  $\text{YbNi}_2\text{B}_2\text{C}$ , a crossover from local moment behavior to an itinerant heavy Fermi liquid is observed. For instance, NMR experiments find that at temperatures above 50 K, both the Knight shift and the nuclear-spin-lattice relaxation rate are accounted for by the presence of localized  $4f$  moments at the  $\text{Yb}^{3+}$  sites, while below 5 K the relaxation rate follows a Korringa relation of a heavy Fermi liquid.<sup>5</sup> Our measurements span a large temperature range that covers both re-

gimes, so different limits of the theory used to explain the magnetotransport in heavy-fermion compounds are required. An analysis of the data based on models suited to either the high- or low-temperature regimes will be given in Sec. III and IV. Finally, the conclusions of our work are discussed in Sec. V.

## II. EXPERIMENTAL PROCEDURE AND RESULTS

The samples measured in this study were grown using a modification of the  $\text{Ni}_2\text{B}$  flux growth technique.<sup>2,6</sup> The constituent elements, with excess Yb to compensate for the loss due to the high vapor pressure of Yb at elevated temperatures, were arc-melted together to form polycrystalline  $\text{YbNi}_2\text{B}_2\text{C}$ . These polycrystalline samples were then slowly cooled with a  $\text{Ni}_3\text{B}$  flux from 1500 to 1200 °C. After cooling to room temperature, single-crystalline plates as large as  $7 \times 7 \times 0.2 \text{ mm}^3$  were obtained with the  $c$  axis perpendicular to the plate surface. Powder  $x$ -ray-diffraction spectra taken on a ground single crystal found a tetragonal lattice structure with  $a = 3.575 \text{ \AA}$  and  $c = 10.606 \text{ \AA}$ , consistent with the lattice parameters reported by Seigrist *et al.*<sup>7</sup>

The magnetoresistance measurements were performed with an 18 T superconducting magnet using a standard four-probe ac technique. The electrical contacts were achieved using  $25.4 \text{ }\mu\text{m}$  platinum wires, and the current was applied along the  $ab$  plane. Experiments above 1.5 K were performed with a variable temperature insert, while a dilution refrigerator was used for measurements down to 50 mK in combination with the 18 T superconducting magnet.

Experiments in pulsed fields up to 50 T with a rise time of 6.5 ms were performed with phase-sensitive detection at a rf frequency of 500 kHz. At high fields, data were collected from  $T = 4 \text{ K}$  down to a base temperature of approximately 500 mK with a  $^3\text{He}$  evaporative cryostat. In the latter case the single-crystalline samples, which were not the same as the ones used for the continuous field measurements, were held in place with epoxy to prevent them from moving during the 50 T pulse. All experiments were performed at the National High Magnetic Field Laboratory in Los Alamos.

The transverse magnetoresistance (i.e.,  $\mathbf{H} \perp \mathbf{I}$ ) was measured with the applied field either perpendicular or parallel to the  $c$  axis of the tetragonal crystal structure. In Fig. 1, the resistance is plotted as a function of temperature for applied fields of zero and 18 T. Notice that the magnetoresistance is negative for  $T > 3 \text{ K}$  and has approximately the same magnitude when the applied field is parallel and perpendicular to the  $c$  axis. These features are also apparent when the normalized magnetoresistance,  $\Delta\rho(H)/\rho(0) = [\rho(H, T) - \rho(0, T)]/\rho(0, T)$ , is plotted as a function of the applied field at different temperatures in Fig. 2. As the temperature is lowered from 60 to 5 K, the magnitude of the magnetoresistance increases.

Below  $\sim 1.6 \text{ K}$ , the electrical resistivity has a Fermi-liquid temperature dependence when the applied field is zero. The temperature range over which Fermi-liquid behavior is observed increases with increasing field (see the insets in Fig. 1). The normalized transverse magnetoresistance at low temperatures is plotted as a function of the applied magnetic field in Fig. 3, and unlike the high-temperature data, it is significantly anisotropic. When the field is perpendicular to

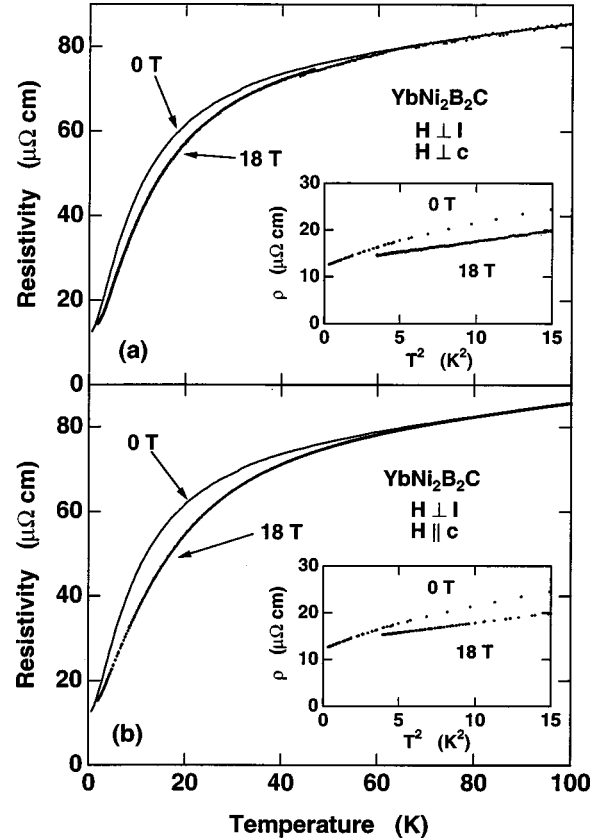


FIG. 1. The resistivity plotted as a function of temperature for  $\text{YbNi}_2\text{B}_2\text{C}$  in zero and 18 T. When the magnetic field was applied perpendicular to the measuring current, it was oriented perpendicular to the  $c$  axis of the tetragonal crystal structure in (a) and parallel to the  $c$  axis in (b). The insets show the resistivity at low temperatures plotted as a function of  $T^2$  for  $H = 0$  and 18 T.

the  $c$  axis, the magnetoresistance is negative down to  $\sim 4 \text{ K}$ . Below this temperature, the magnetoresistance is initially positive and then turns negative at higher fields, creating a maximum. This maximum gradually moves to higher fields as the temperature is decreased to  $T = 1.6 \text{ K}$ , where it is at  $\sim 10 \text{ T}$ . The data are qualitatively different when the magnetic field is parallel to the  $c$  axis. At all temperatures above 1.7 K, the magnetoresistance is always negative, and as the temperature is lowered, a local minimum develops around 8 T. In Fig. 4, the very-low-temperature data taken with a dilution refrigerator in the 18 T magnet are presented for  $\mathbf{H} \perp \mathbf{c}$ .

Higher field data for  $\mathbf{H} \perp \mathbf{c}$ , which were measured while the field was increasing on the pulsed magnet, are shown in Fig. 5. Notice that at the lowest temperature, the maximum in the magnetoresistance is no longer moving to higher fields with decreasing temperature, and in fact it is at a slightly lower field when  $T = 500 \text{ mK}$  in comparison to the data taken at  $T = 1.2 \text{ K}$ . For fields above 25 T, an inflection point is found at all temperatures below 4 K. This tendency gets stronger as the temperature is lowered, resulting in a peculiar crossing of the magnetoresistance curves for the lowest two measurement temperatures. The eventual development of a small positive magnetoresistive component at the highest fields for  $T = 500 \text{ mK}$  may be associated with cyclotron orbit effects.

It should be noted that the experiments with the variable-

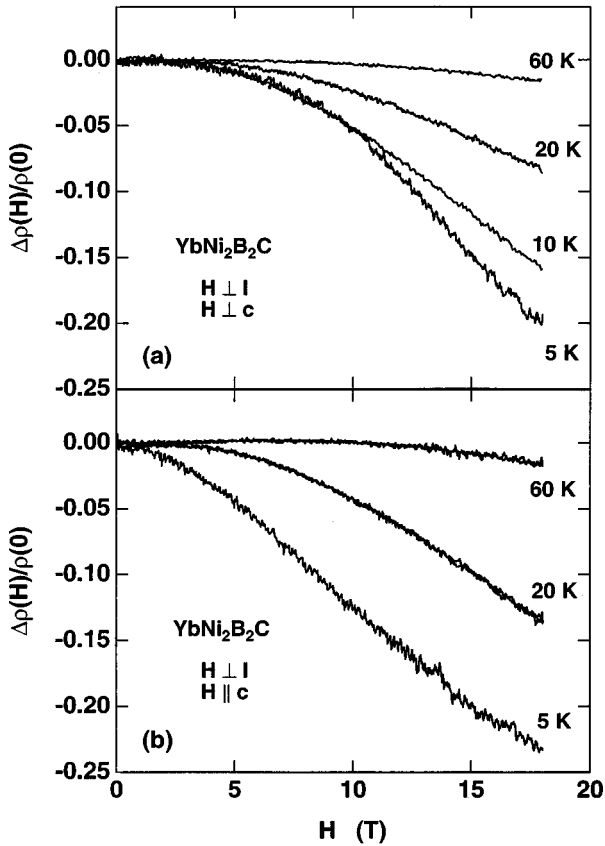


FIG. 2. The normalized transverse magnetoresistance,  $\Delta\rho(H)/\rho(0)=[\rho(H,T)-\rho(0,T)]/\rho(0,T)$ , vs the applied magnetic field at several different temperatures between 5 and 60 K for  $\text{YbNi}_2\text{B}_2\text{C}$ . The field direction is perpendicular and parallel to the  $c$  axis in (a) and (b), respectively.

temperature insert in the 18 T magnet, the dilution refrigerator in the 18 T magnet, and the He-3 cryostat in the pulsed magnet were performed on three different samples. While the three different data sets are qualitatively alike in the temperature and field ranges where they overlap, varying impurity contributions and slightly different field alignments may account for the quantitative discrepancies. Since the high- and low-temperature analyses are independent of each other, we do not believe these variations will effect our conclusions.

Finally, because the conduction-electron scattering depends on the degree of polarization for the localized moments, the magnetization was measured up to 18 T. These measurements were performed with a vibrating-sample magnetometer in the 18 T superconducting magnet, and the data at  $T=1.7$  K are displayed in Fig. 6 with the applied field perpendicular and parallel to the  $c$  axis. The anisotropy in  $M(T,H)$  shown here is consistent with the magnetic anisotropy seen at higher temperatures.<sup>3</sup>

### III. MAGNETOTRANSPORT AT HIGH TEMPERATURES

The features observed in the high-temperature magnetoresistance of  $\text{YbNi}_2\text{B}_2\text{C}$  are similar to other heavy-fermion compounds and qualitatively consistent with a reduction of spin-disorder scattering as the moments are polarized. For spin-disorder scattering the magnetoresistance  $\rho(H)\sim[1$

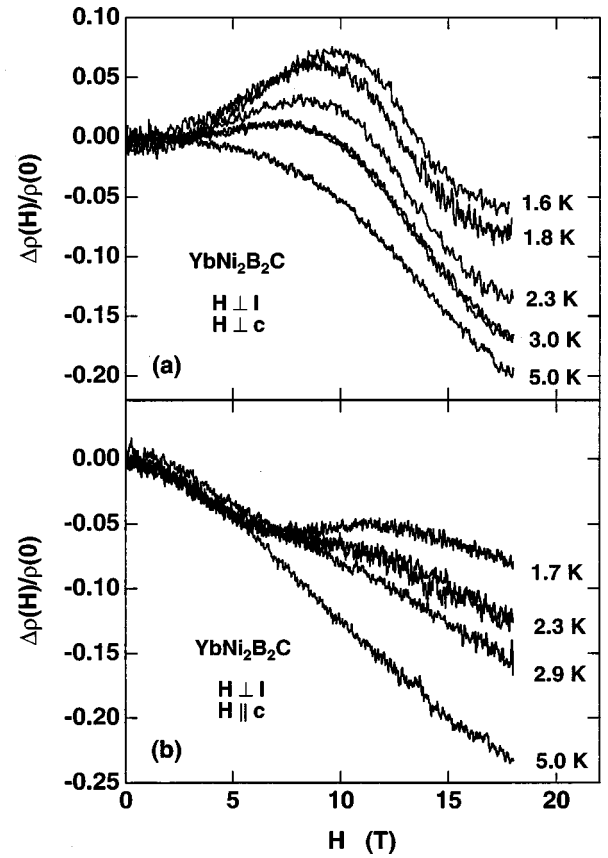


FIG. 3. The normalized transverse magnetoresistance,  $\Delta\rho(H)/\rho(0)=[\rho(H,T)-\rho(0,T)]/\rho(0,T)$ , vs the applied magnetic field at low temperatures for  $\text{YbNi}_2\text{B}_2\text{C}$ . The field direction is perpendicular and parallel to the  $c$  axis in (a) and (b), respectively.

$-\langle S \rangle^2]$ , where  $\langle S \rangle$  is the normalized thermal-average spin moment.<sup>8</sup> Since  $\langle S \rangle$  is proportional to the magnetization, the low-field limit of the normalized magnetoresistance should be  $\sim -H^2$ . This field dependence is not observed [see Eq. (1) below], and attempts to scale the normalized magnetore-

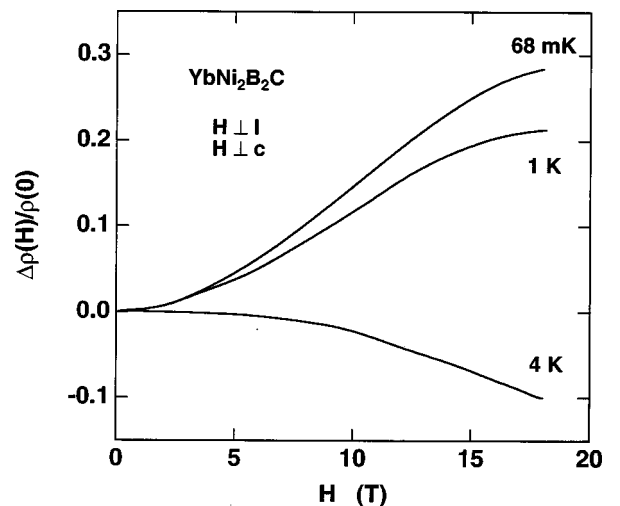


FIG. 4. The transverse magnetoresistance,  $\Delta\rho(H)/\rho(0)=[\rho(H,T)-\rho(0,T)]/\rho(0,T)$ , vs the applied magnetic field for  $\text{YbNi}_2\text{B}_2\text{C}$ . A dilution refrigerator in the 18 T magnet was used to collect these data with the field perpendicular to the  $c$  axis.

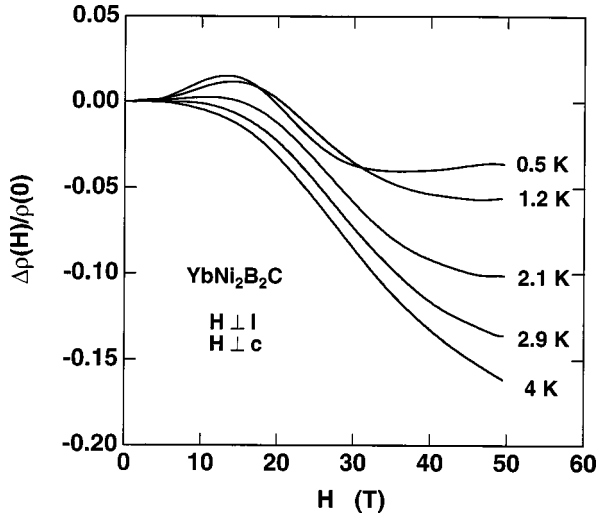


FIG. 5. The transverse magnetoresistance,  $\Delta\rho(H)/\rho(0) = [\rho(H,T) - \rho(0,T)]/\rho(0,T)$ , plotted up to 50 T for  $\text{YbNi}_2\text{B}_2\text{C}$  at several temperatures between 0.5 and 4 K. These data were measured using a pulsed magnet with the field direction perpendicular to the  $c$  axis of the tetragonal crystal structure.

sistance with the measured field-dependent magnetization only qualitatively explain the data.

Even though the formal justification may be lacking, single-impurity models are often used to analyze data for heavy-fermion compounds at high temperatures where localized electrons appear to respond independently of each other. The magnetoresistance for the single impurity can be calculated from the scattering phase shifts of the conduction electrons using an expression derived from a sum rule. The phase shift depends on the magnetization, and with the Coqblin-Schrieffer model, the solution for the magnetoresistance is a universal function of  $H/T_K$ , where  $T_K$  is the Kondo temperature. When the negative of the normalized magnetoresistance versus field for  $\mathbf{H} \perp \mathbf{c}$  is displayed on a log-log plot in Fig. 7, a series of parallel lines are obtained for different temperatures above 5 K, implying that it is possible to scale

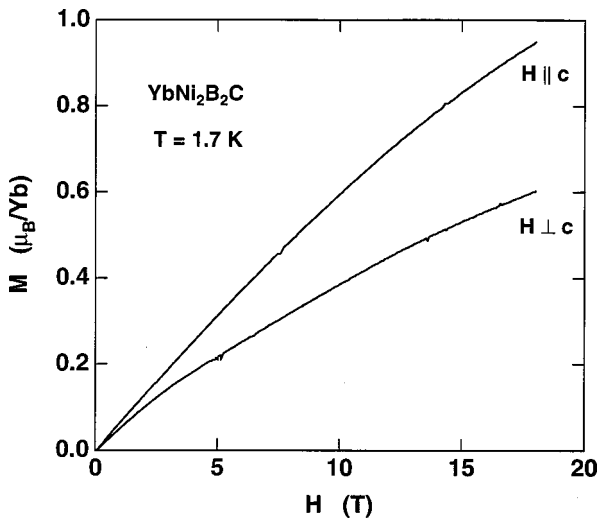


FIG. 6. The magnetization  $M$  as a function of the applied magnetic field  $H$  both parallel and perpendicular to the  $c$  axis for  $\text{YbNi}_2\text{B}_2\text{C}$ . The sample temperature was 1.7 K.

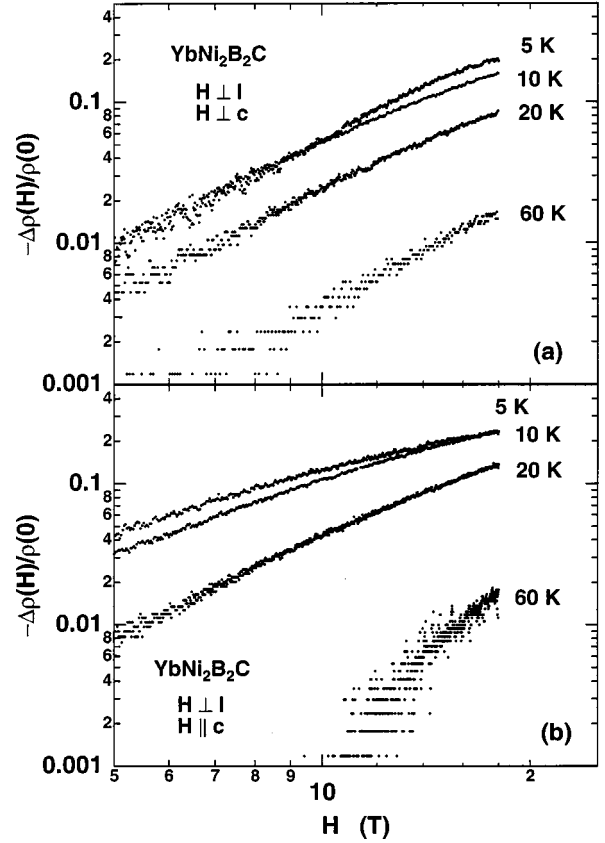


FIG. 7. The normalized transverse magnetoresistance vs the applied magnetic field on a log-log plot for  $\text{YbNi}_2\text{B}_2\text{C}$ . The data were measured with the field (a) perpendicular and (b) parallel to the  $c$  axis at several temperatures above 5 K. The digital noise, when  $-\Delta\rho(H)/\rho(0)$  is small at low fields, is an artifact of the instrument used to measure the resistance.

the applied magnetic field in such a way that the high-temperature data all follow a common function. The small values of  $-\Delta\rho(H)/\rho(0)$  at low fields are discrete, and this digital noise is an artifact of the instrument used to measure the resistance. Notice that the scaling starts to break down at high fields for the 5 K data. This represents a crossover to a low-temperature regime, which will be discussed in the next section. One possibility is to scale the magnetoresistance to the prediction of the spin- $\frac{1}{2}$  single-impurity Kondo model, which is given by the empirical relation  $\rho(H)/\rho(0) = [1 + (\mu_B H/k_B T_K)^2]^{-1/2}$  and is represented by the solid line in Fig. 8.<sup>9</sup> Unfortunately our low-field data follow the expression

$$-\Delta\rho(H)/\rho(0) = \beta(\mu_B H/k_B T_H)^\alpha, \quad (1)$$

where  $\alpha = 2.8$ ,  $\beta = 3.7$ , and  $T_H$  depends on the measurement temperature (see below), while for the single-impurity model  $\Delta\rho(H)/\rho(0) \sim -H^2$ . Unlike the heavy-fermion system  $\text{UBe}_{13}$ , where  $\alpha = 1.6$ , the  $\alpha$  for  $\text{YbNi}_2\text{B}_2\text{C}$  is greater than 2. Following this procedure, a characteristic temperature  $T_H$  was determined for  $\text{YbNi}_2\text{B}_2\text{C}$  at each measurement temperature by scaling the applied field so that the low-field data overlap the single-impurity prediction, as indicated in Fig. 8. From the inset in Fig. 8,  $T_H = T + T_0$ , where  $T_0 \sim 20$  K. Thus the characteristic temperature for  $\text{YbNi}_2\text{B}_2\text{C}$  depends linearly

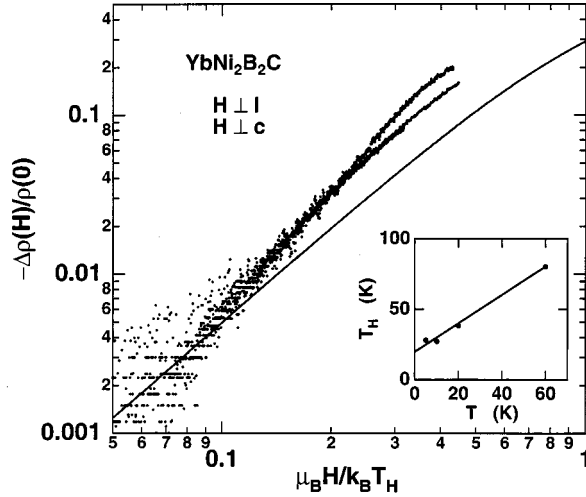


FIG. 8. The normalized transverse magnetoresistance plotted as a function of the dimensionless parameter  $\mu_B H / k_B T_H$ , where the characteristic temperature  $T_H$  is scaled so that the low-field data coincide with the prediction of the spin- $\frac{1}{2}$  single-impurity Kondo model given by the empirical relation  $1 - [1 + (\mu_B H / k_B T_H)^2]^{-1/2}$  (the solid line). The inset shows how  $T_H$  varies with measurement temperature, and the solid line is  $T_H = T + 20$  K.

on the measurement temperature and extrapolates to a value that is approximately a factor of 2 larger than the Kondo temperature determined by low-temperature thermodynamic measurements. If the magnetoresistance data are scaled to some other universal function (e.g., adjusting the high-field data to correspond with the theoretical prediction for the single impurity model), the slope between the characteristic and measurement temperatures is no longer 1, and there is a small change in the intercept  $T_0$ . Since a series of parallel lines are not obtained in Fig. 7(b), this type of scaling analysis is not possible with the data for  $\mathbf{H} \parallel \mathbf{c}$ .

Kawatami and Okiji used the single-site approximation for the Anderson lattice to calculate  $\Delta\rho(H)/\rho(0)$  as a function of temperature.<sup>10</sup> In this calculation, the phase shift at each site for the perfect lattice at  $T=0$  is equal to the unitarity limit. Thermal fluctuations in the phase shift then cause the scattering rate to increase, while the applied magnetic field reduces the fluctuations by polarizing the moments. At lower temperatures, the magnetoresistance can become positive because of the gap structure in the Kondo resonance just above the Fermi level. In Fig. 9, the normalized magnetoresistance,  $\Delta\rho(18\text{ T})/\rho(0) = [\rho(18\text{ T}, T) - \rho(0, T)]/\rho(0, T)$ , at  $H=18\text{ T}$  is plotted as a function of temperature, and these data semiquantitatively agree with the calculation in Fig. 3 of Ref. 10. For a minimum in  $\Delta\rho(18\text{ T})/\rho(0)$  of  $-0.2$ ,  $T_K \sim g\mu_B H / (k_B 0.6) \sim 20\text{ K}$  if  $g=1$ . Not only is this estimate of the Kondo temperature the same as the value found from the scaling analysis above, but the minimum in the data occurs at  $T \sim 4\text{ K}$ , which is reasonably close to  $T_K/4$  where the theory predicts. The effects of cyclotron orbits on the magnetoresistance were not corrected for in this analysis. These will tend to increase the resistance and our estimate of the Kondo temperature.

Finally, when the scattering mechanism for the different types of charge carriers is the same, the magnetoresistance should obey Kohler's rule,<sup>8</sup>

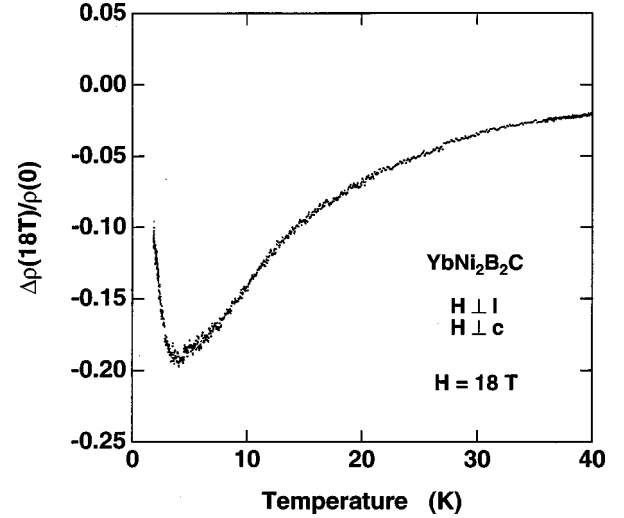


FIG. 9. The normalized transverse magnetoresistance,  $\Delta\rho(18\text{ T})/\rho(0) = [\rho(H=18\text{ T}, T) - \rho(0, T)]/\rho(0, T)$ , vs temperature for  $\text{YbNi}_2\text{B}_2\text{C}$ . The field direction is perpendicular to the  $c$  axis.

$$\Delta\rho(H, T)/\rho(0, T) = f(H/\rho(0, T)). \quad (2)$$

If the normalized magnetoresistance were plotted as a function of  $H/\rho(0, T)$  instead of  $H/T_H$  in Fig. 8, the figure would represent a Kohler plot of the data. However, for  $\text{YbNi}_2\text{B}_2\text{C}$  the data do not follow Kohler's rule because the scaling is obtained with  $T_H$ , which is not proportional to  $\rho(0, T)$ . This is not unexpected for a system with a field-dependent scattering rate.

#### IV. MAGNETOTRANSPORT IN THE FERMI-LIQUID REGIME

The scaling behavior observed in Sec. III, holds above a low-temperature cutoff, which depends weakly on the applied field [i.e.,  $T_{c0}(11\text{ T}) \sim 6\text{ K}$  and decreases to  $\sim 3.6\text{ K}$  for  $H=18\text{ T}$ ].

Below the cutoff in the Fermi-liquid regime, the magnetoresistance, which has a residual term due to disorder and a temperature-dependent term from electron-electron interactions, can be expressed as

$$\rho(H) = \rho_0(H) + A(H)T^2, \quad (3)$$

where  $\rho_0$  and  $A$  depend on the applied magnetic field. Several theoretical treatments of the magnetic-field dependence of the residual resistivity have been reported.<sup>11-13</sup> Two types of disorder exist in heavy-fermion compounds: Kondo-hole disorder associated with substitutional impurities on the  $f$ -electron sites and ligand disorder from impurities on the intermetallic ion sites. The antiferromagnetic exchange interaction, which is responsible for the heavy Fermi liquid at low temperatures, depends on both the degree of hybridization between the localized and conduction electrons and the position of the  $f$ -electron energy level relative to the Fermi energy. The type of disorder effects the exchange interaction in different ways. For Kondo-hole disorder, the impurities modify the potential at the substituted  $f$  sites, while the impurities on the conduction-electron sites vary the hybridization. In either case, the exchange interaction is changed, and depending on the kind of disorder, the system will respond

differently to an applied magnetic field. Using a slave-boson mean-field theory, which includes correlations between the different  $f$  sites unlike Ref. 11, Chen *et al.* examined the effects of disorder in the two-conduction-band Anderson lattice Hamiltonian where the applied magnetic field was introduced as a Zeeman term in the energies of the conduction and  $f$  electrons.<sup>12,13</sup> As the applied field is increased, the residual resistivity due to ligand disorder initially increases dramatically before going through a maximum and then decreasing to a value that is close to what it had at zero field. For Kondo-hole disorder, the residual resistivity always decreases with increasing field. From a large- $N$  expansion of the Anderson lattice Hamiltonian,<sup>14</sup> one finds that the quadratic-temperature dependence is a consequence of charge fluctuations. The  $T^2$  coefficient  $A$  for the temperature-dependent contribution to the resistivity is proportional to the square of the density of quasiparticle states evaluated at the Fermi energy, and this monotonically decreases with increasing field.

In actual compounds, both types of impurities are present and uncorrelated in the dilute limit. The two types of disorder in addition to the temperature-dependent term can produce a nonmonotonic field dependence for the magnetoresistance at very low temperatures with a maximum at a finite field. Hence the local maximum is a consequence of the competition between the impurity effects and charge fluctuations. As the temperature is increased, the resistivity curves continuously evolve to a monotonically decreasing behavior as the maximum at finite fields moves to lower and lower fields (see Fig. 3 in Ref. 12). If the amount of Kondo-hole disorder is significant, then the high-field resistivity can be lower than the zero field value.

For  $\mathbf{H} \perp \mathbf{c}$ , the low-temperature transverse magnetoresistance is qualitatively similar to what the theory predicts, and it is possible to extract the field dependence of  $A$  and  $\rho_0$  from these data. Both of these coefficients normalized by their zero-field values are plotted in Fig. 10. Notice that the quadratic temperature coefficient decreases with increasing field, consistent with the theoretical expectation. A phenomenological model can be used to extract a characteristic energy scale from the field dependence of  $A$ . Assume the density of states is a Lorentzian centered on the Fermi energy with a full width at half maximum equal to some characteristic energy  $2T_0$ , and the field dependence is included by a Zeeman splitting of the Lorentzian by  $2\mu_B H$ . The coefficient  $A$  is then proportional to the square of the density of states. Using this model, a reasonable fit to the measured  $A$  is obtained [the solid line in Fig. 10(a)] with  $T_0 \sim 12$  K. A slightly better fit was obtained with a similar energy scale when an additional parameter was introduced that allowed the Lorentzian to be shifted from the Fermi energy; however, the difference was judged to be experimentally insignificant. Even though this unrefined model neglects any field dependence of the Kondo resonance's spectral weight,  $T_0$  is fairly close to the thermodynamically determined Kondo temperature of 10 K.

Over the same field range,  $\rho_0$  monotonically increases, never reaching the maximum that is theoretically anticipated when ligand disorder is present [see Fig. 10(b)]. The maximum in  $\rho_0$  occurs where the applied field produces a magnetization in the sample that is half its saturation value. From Fig. 6 the magnitude of the magnetization at 18 T for  $\mathbf{H} \perp \mathbf{c}$  is

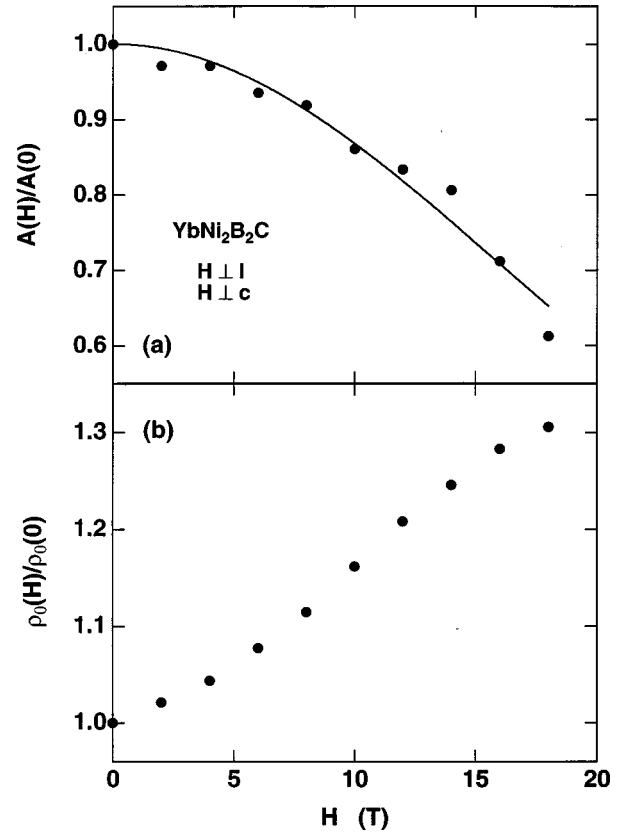


FIG. 10. (a) The normalized coefficient of the  $T^2$  term for the resistivity in the low-temperature Fermi-liquid regime vs the applied magnetic field for  $\text{YbNi}_2\text{B}_2\text{C}$ . The solid line is a fit to a phenomenological model described in the text. (b) The magnetic field dependence of the normalized residual resistivity determined by extrapolating the low-temperature data to zero. The field was applied in a direction perpendicular to the  $c$  axis.

approximately half the value when  $\mathbf{H} \parallel \mathbf{c}$ , which is still not saturated. Hence at 18 T the magnetization for  $\mathbf{H} \perp \mathbf{c}$  must be less than half its saturation value, and the absence of a peak in the field dependence of  $\rho_0$  is reasonable.

Presently, the theoretical treatment of magnetoresistance has not considered the consequences of anisotropy in a quantitative manner, and the theoretical predictions are qualitatively different from the measured magnetoresistance when  $\mathbf{H} \parallel \mathbf{c}$ . In fact, if a molecular field is present, the magnetotransport is a universal function of the magnetization, not the applied field. When dealing with systems that have a significant anisotropy energy, it is informative to compare the magnetoresistance for the different field directions at the same value of magnetization. For  $\text{YbNi}_2\text{B}_2\text{C}$ , the magnetization at 18 T when  $\mathbf{H} \perp \mathbf{c}$  is comparable to that at  $\sim 7$  T when  $\mathbf{H} \parallel \mathbf{c}$ . Above 1.7 K, the magnetoresistance for  $\mathbf{H} \parallel \mathbf{c}$  monotonically decreases with increasing field up to 7 T. It is possible that for this field direction, the crossover into a regime of positive magnetoresistance lies below 1.7 K, and the local maximum at higher fields is unrelated to the Kondo interaction.

## V. CONCLUSION

In the rare-earth borocarbide series,  $\text{YbNi}_2\text{B}_2\text{C}$  is an interesting member because it is the only one that does not

have a ground state with long-range order. Instead, a heavy Fermi liquid develops at low temperatures where the Kondo temperature is well separated from other energy scales in the system, making  $\text{YbNi}_2\text{B}_2\text{C}$  an ideal system to study how large magnetic fields effect the Kondo-type interactions.

In this paper the transverse magnetoresistance was reported over a wide temperature range. At high temperatures, the magnetoresistance is negative, and its magnitude increases as the temperature is lowered. When the applied field is perpendicular to the  $c$  axis,  $\Delta\rho(H)/\rho(0)$  decreases more quickly than the quadratic dependence expected from theoretical considerations; however, it is still possible to scale these data. From this analysis, a characteristic temperature  $T_H$  is found, which increases linearly with the measurement temperature and has a zero-temperature intercept of  $\sim 20$  K. The magnetoresistance is anisotropic, and a scaling analysis was not possible for the data taken with the field parallel to the  $c$  axis.

This scaling also breaks down at low temperatures, and the properties eventually evolve into those of a Fermi liquid. In the Fermi-liquid regime, the resistivity has a residual term due to impurities and a temperature-dependent term from electron-electron scattering. Both the residual contribution and the  $T^2$  coefficient depend on the applied field in a fashion qualitatively consistent with theoretical expectations. By simply modeling the Kondo resonance with a Lorentzian that is split with a Zeeman energy from the applied field, a characteristic energy of  $\sim 12$  K was determined. The residual resistivity was found to increase with field up to 18 T, which

should occur when ligand disorder dominates over Kondo-hole disorder.

Qualitatively, our results are consistent with theoretical calculations based on the periodic Anderson model. When compared to specific predictions from this model or a phenomenological counterpart, the characteristic energy obtained from the fit is typically a factor of 2 larger than the Kondo temperature determined from the Sommerfeld coefficient. Also a more precise calculation is needed for the transition from the high-temperature scaling regime to the low-temperature Fermi-liquid regime, and no explanation exists for the greater than quadratic field dependence of the magnetoresistance at high temperatures. Finally, the magnetoresistance for the field parallel to the  $c$  axis is different from the data with the field in the perpendicular direction, and at this time this anisotropy has not been seriously accounted for in theoretical treatments.

#### ACKNOWLEDGMENTS

We wish to thank G. M. Schmiedeshoff for his assistance on some of the measurements. This work was supported by the National Science Foundation under Grant No. DMR-9624778 and the Director for Energy Research, Office of Basic Energy Science at the U.S. Department of Energy. The work at the NHMFL–Pulsed Field Facility was performed under the auspices of the National Science Foundation, State of Florida, and the U.S. Department of Energy. Ames Laboratory is operated for the U.S. Department of Energy by Iowa State University under Contract No. W-7405-ENG-82.

<sup>1</sup>R. Nagarajan *et al.*, Phys. Rev. Lett. **72**, 274 (1994); R. J. Cava *et al.*, Nature (London) **376**, 252 (1994); B. K. Cho, P. C. Canfield, and D. C. Johnston, Phys. Rev. B **52**, 3844 (1995); P. C. Canfield, P. L. Gammel, and D. J. Bishop, Phys. Today **51** (10), 40 (1998).

<sup>2</sup>A. H. Lacerda *et al.*, Philos. Mag. B **74**, 641 (1996).

<sup>3</sup>A. Yatskar *et al.*, Phys. Rev. B **54**, R3772 (1996); S. K. Dhar *et al.*, Solid State Commun. **98**, 985 (1996).

<sup>4</sup>Z. Fisk *et al.*, Phys. Rev. Lett. **61**, 3310 (1991); R. Robinson *et al.*, *ibid.* **75**, 1194 (1995).

<sup>5</sup>R. Sala *et al.*, Phys. Rev. B **56**, 6195 (1997).

<sup>6</sup>B. K. Cho *et al.*, Phys. Rev. B **52**, 3684 (1995); M. Xu *et al.*,

Physica C **227**, 321 (1994).

<sup>7</sup>T. Siegrist *et al.*, Nature (London) **376**, 254 (1994).

<sup>8</sup>P. L. Rossiter, *The Electrical Resistivity of Metals and Alloys* (Cambridge University Press, Cambridge, 1987).

<sup>9</sup>T. Graf *et al.*, Phys. Rev. B **52**, 3099 (1995).

<sup>10</sup>N. Kawakami and A. Okiji, J. Phys. Soc. Jpn. **55**, 2114 (1986).

<sup>11</sup>F. J. Ohkawa, J. Phys. Soc. Jpn. **55**, 2527 (1986); Phys. Rev. Lett. **65**, 2300 (1990).

<sup>12</sup>C. Chen, Z.-Z. Li, and W. Xu, J. Phys.: Condens. Matter **5**, 95 (1993).

<sup>13</sup>C. Chen and Z.-Z. Li, J. Phys.: Condens. Matter **6**, 2957 (1994).

<sup>14</sup>A. J. Millis and P. A. Lee, Phys. Rev. B **35**, 3394 (1987).